Capillarity

Vol. 17, No. 3, p. 81-96, 2025

Original article

The key role of hydroxyl in thermal transport at the silica-water interface: A molecular dynamics simulation

Ming Ma[1], Jifan Li[2,3], Xiaohui Zhang[2,3]*, Shan Qing[2,3]

[1]*School of Nationality Educators, Qinghai Normal University, Xining 810016, P. R. China*

[2]*State Key Laboratory of Complex Nonferrous Metal Resources Clean Utilization, Kunming University of Science and Technology, Kunming 650093, P. R. China*

[3]*Faculty of Metallurgy and Energy Engineering, Kunming University of Science and Technology, Kunming 650093, P. R. China*

Keywords:
Silica-water interface
thermal boundary conductance
molecular dynamics
interfacial thermal transport
hydrogen bonds
vibrational density of states

Cited as:
Ma, M., Li, J., Zhang, X., Qing, S. The key role of hydroxyl in thermal transport at the silica-water interface: A molecular dynamics simulation. Capillarity, 2025, 17(3): 81-96.
https://doi.org/10.46690/capi.2025.12.02

Abstract:
A comprehensive understanding of thermal transport across solid-liquid interfaces is crucial for enhancing the performance of micro- and nanoscale devices, especially at the silica-water interface, which plays a key role in many applications in energy conversion and medical technologies. The adsorbed water layer at the silica interface plays a core role in solid-liquid interface thermal transport. However, the molecular-level structural transitions of this layer and their correlation with thermal transport mechanisms have not been extensively studied. In this work, molecular dynamics simulations were used to study the thermal transport mechanisms at silica-water interfaces with different hydroxyl densities, focusing on how interfacial H-bonds and layered structures influence interfacial thermal transport characteristics. The results of the study show that the interfacial thermal conductance increases with the hydroxyl density, while the density distribution of water molecules at the silica interface shows an opposite trend. The formation of H-bonds at the interface is identified as the main cause of this anomalous behavior. Through density, charge, H-bonds, and water molecule orientation distribution, the bilayer structure of the adsorbed water layer at the silica interface was defined at the molecular level, which is composed of the binding interface layer and the diffuse layer. The binding interface layer plays a decisive role in interfacial thermal transport. Through the analysis of interfacial potential energy, H-bonds dynamics, and Vibrational density of states, the microscopic mechanisms of thermal transport at silica-water interfaces with different hydroxyl densities were proposed by this work. These findings may provide new insights into the understanding of thermal transport mechanisms at solid-liquid interfaces.

1. Introduction

The silica-water interface, as a representative solid-liquid interface, is ubiquitous in applications such as solar thermal applications (Bahiraei et al., 2020; Qi et al., 2024), polymer composite materials (Idumah and Obele, 2021; Zhao et al., 2024), interfacial evaporation (Kieu et al., 2018; Liang et al., 2024), Seawater Desalination (Zhang and Su, 2018; Chen et al., 2021) and micro/nano heat sinks (Huang et al., 2023). However, when the characteristic dimensions of the structure are close to the nanoscale, the thermal resistance generated by the interface accounts for a significant portion, if not dominates, the overall heat transfer process (Wu and Han, 2022). Hence, elucidating the microscopic heat transfer mechanisms

Yandy Scientific Press

*Corresponding author.
E-mail address: mm0317ky@163.com (M. Ma); jifan0017@gmail.com (J. Li); xiaohui.zhang@kust.edu.cn (X. Zhang); m15087088903@163.com (S. Qing).

Received September 28, 2025; revised October 19, 2025; accepted November 7, 2025; available online November 10, 2025.

at the nano-silica and water interface is crucial for enhancing and optimizing the performance of silica in various technological domains. Research related to heat transport across solid-liquid interfaces originated with Kapitza's investigation into the flow of ^{4}He (helium II) at low temperatures, where a temperature discontinuity was observed upon thermal transport through the interface (Kapitza, 1941). This discontinuity leads to thermal boundary resistance, also known as Kapitza resistance, which is defined by the relation $q = \Delta T / R_k$, where q represents heat flux and ΔT is the temperature jump at the interface. Alternatively, some researchers prefer to consider the reciprocal of thermal boundary resistance, commonly referred to as thermal boundary conductance (TBC) (Chen et al., 2022).

Research on TBC has shown that at solid-liquid interfaces, not only is there a temperature jump, but the structure and dynamics of the liquid also undergo significant changes (Wang et al., 2024). Liquid molecules are readily adsorbed onto the solid surface, forming a layer that is often described as a "bridge" for heat transport across the interface (Xue et al., 2004). Current studies focus on methods to induce the formation of a stable adsorbed layer on solid surfaces by manipulating factors such as interface temperature (Barisik and Beskok, 2014), wettability (Gao et al., 2022; Ma et al., 2024), roughness (Wang and Keblinski, 2011; Huang et al., 2022), patterning (Ueki et al., 2022), functionalization, and surface charge (Wang et al., 2018). For example, experimental results show that functionalizing silica nanoparticle surfaces significantly enhances interfacial thermal transport, which is attributed to abnormal density stratification at the nanoparticle interface (Kodama et al., 2021). A deeper understanding of the structural transitions and density stratification of water molecules at solid-liquid interfaces is crucial for explaining the microscopic mechanisms of heat transport and optimizing the design of solid surfaces.

Earlier studies aimed at understanding the structural changes of water molecules at the silica interface have employed techniques such as X-ray diffraction (Morishige, 2018) and atomic force microscopy (Pittenger et al., 2001). These studies revealed that H-bonds between water molecules and hydroxyl groups on the silica surface contribute to the formation of an ice-like structure, which plays a key role in the structural transition of water at the interface. However, due to limitations in experimental precision, the molecular-level details of the silica-water interface, particularly the structural characteristics and precise nature of the adsorbed water layer, remain unclear. Recently, significant advancements have been made in studying the silica-water interface through nonlinear spectroscopic methods, particularly vibrational sum frequency generation (SFG) spectroscopy. Pezzotti et al., 2019 used SFG in combination with density functional theory simulations to examine the ordered and disordered states of interfacial water molecules. They identified two distinct layers: A binding interfacial layer (BIL) and a diffusion layer (DL), with SFG signals being decomposed and analyzed based on this layered structure. Furthermore, by comparing the crystalline quartz/water interface with the amorphous silica/water interface, they established a relationship between surface crystallinity and the interfacial structure, along with its spectral properties. These findings have provided valuable insights into the microstructural features of the silica-water interface.

The molecular dynamic (MD) simulations have become an essential tool for studying the structural and dynamic behaviors of the silica-water interface. These simulations cover a wide range of phenomena, such as interfacial freezing (Uchida et al., 2021), wettability transitions (Jin et al., 2020), diffusion behaviors (Milischuk and Ladanyi, 2011), the effect of silanol groups on water molecules (Sun et al., 2023), and pore flow (Bourg and Steefel, 2012). Together, these studies show that H-bonds are a key factor in determining the structural properties of water molecules at the interface. However, relatively few studies based on MD simulations have examined the structural features of water molecules at the silica interface. Moreover, most existing research has focused on the adsorbed water layer's structural characteristics, with limited exploration into its relationship with energy transfer. As the characteristic scale shrinks to the nanometer range, the unique polarity of water molecules and the presence of hydroxyl groups on the silica interface disrupt the H-bond network in the interfacial water molecules, leading to restricted diffusion and altered dipole angle distributions. As a result, the structural transitions and layering behavior of the adsorbed water layer, as well as the formation of H-bonds, play a significant role in heat transfer at the solid-liquid interface. For instance, Schoen et al. (2009) showed through MD simulations that the hydrophilic silanol-water interface exhibits better thermal transport efficiency than the hydrophobic silane-water interface, attributed to H-bonds between the silanols and water. Their findings also revealed that TBC decreases with temperature, which is attributed to a reduction in the number of H-bonds. Similarly, Sun et al. (2024) demonstrated that increased surface ionization enhances TBC by strengthening hydrogen bonding between ionized silica and water, thus improving heat conduction. Moreover, Hu et al. (2009) used non-equilibrium molecular dynamics (NEMD) to investigate thermal rectification at the silica-self-assembled monolayer-water interface. Schoen et al. (2009) also found that the TBC of hydrophilic silanols is temperature and time-dependent, whereas the TBC of hydrophobic silanols remains constant, highlighting the important role of the H-bond network in these processes.

However, to the best of our knowledge, few studies have considered interfacial thermal transport between the silica-water interface with varying hydroxyl coverage. In practice, when silica surfaces are exposed to air or aqueous environments, water reacts with the surface to form silanol groups. The polarity and degree of hydroxylation of the silica surface directly influence its wettability. Thus, the tunable degree of hydroxylation on silica surfaces gives rise to complex and variable surface properties, which in turn significantly affect interfacial thermal transport. Therefore, exploring the effect of interfacial thermal transport between silica surfaces with different hydroxylation degrees and water holds important practical significance. The scarcity of previous research in this field also serves as the primary motivation for the present study.

The aim of this study is to explore the thermal transport

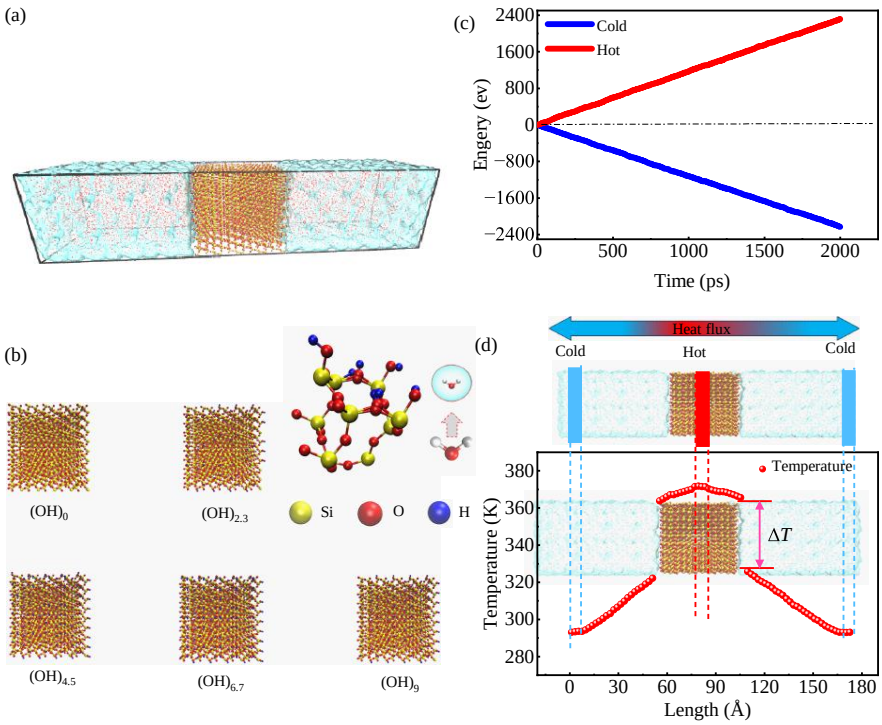

Fig. 1. (a) MD simulation system, (b) schematic of silica surfaces with varying hydroxyl densities, (c) heat flux, and (d) temperature gradient.

mechanisms at silica-water interfaces with varying hydroxyl densities, focusing on how interfacial H-bonds and layering structures influence heat transfer. To achieve this, MD simulations were conducted to create five silica models with different hydroxyl densities. The study analyzed the density, charge, H-bond formations, and water molecule orientations to understand the bilayer structure of the adsorbed water layer at the silica interface. Additionally, the interfacial potential energy, H-bond dynamics, and vibrational density of states were examined to investigate the microscopic mechanisms of thermal transport at these interfaces. The results aim to provide insights into the thermal transport mechanisms at silica-water interfaces, offer theoretical support for the design of silica-based nanomaterials, and advance their applications in the energy sector. The paper is structured as follows: Section II details the computational methods used in the simulations; Section III discusses the structural characteristics of water molecules at silica interfaces with varying hydroxyl densities and the associated microscopic thermal transport mechanisms; and Section IV concludes with a summary of the findings.

2. Computational methodology

2.1 Model establishment

2.1.1 Establishment of silica with varying hydroxyl densities

Silica surfaces with varying hydroxyl densities were generated using CHARMM (Emami et al., 2014), with the initial dimensions of the silica walls set at 40.315 Å × 41.432 Å × 47.608 Å. The surfaces were hydroxylated with silanol groups exhibiting different area number densities. For ease of reference, these surfaces were designated as $(OH)_0$, $(OH)_{2.3}$, $(OH)_{4.5}$, $(OH)_{6.7}$, and $(OH)_9$, respectively. In the notation $SiO_2(OH)_n$, the variable n denotes the area density of hydroxyl on the silica surface, which is calculated by dividing the number of hydroxyl groups by the area of the x-y surface. A schematic representation of the model is provided in Fig. 1(b).

2.1.2 Modeling of thermal transport at the SiO_2-water interface

Fig. 1(a) presents a schematic diagram of the simulation setup used in this study. In this model, silica walls with varying levels of hydroxylation are placed at the center of the simulation box, with water molecules positioned on either side. The H_2O are modeled at a density of 998 kg/m^3, which corresponds to a temperature of 293 K, and are randomly distributed around the SiO_2 walls using the Packmol software (Martínez et al., 2009). The interactions between atoms in the silica are defined by the CHARMM force field, and the associated potential function is given as follows (Emami et al., 2014):

$$E_{\text{pot}} = \sum_{ij,\text{nonbonded 1,2 and 1,3 excl}} \varepsilon_{ij}\left[2\left(\frac{\sigma_{ij}}{r_{ij}}\right)^9 - 3\left(\frac{\sigma_{ij}}{r_{ij}}\right)^6\right] + \frac{1}{4\pi\varepsilon_0}\sum_{ij,\text{nonbonded 1,2 and 1,3 excl}}\frac{q_i q_j}{r_{ij}} + \sum_{ij,\text{bonded}} k_{i,ij}\left(r_{ij}-r_{0,ij}\right)^2 + \sum_{ijk,\text{bonded}} k_{\theta,ijk}\left(\theta_{ijk}-\theta_{0,ijk}\right)^2 \quad (1)$$

Table 1. Nonbonded parameters for SiO_2 and hydroxylated SiO_2 surfaces.

Atom	ε_{ij} (Kcal/mol)	σ_{ij} (Å)	Charge (e)
Si	0.093	4.15	+1.1 +0.725α
O^{Si}	0.054	3.47	-0.55
O^{H}	0.122	3.47	-0.675
O^{Bare}	0.122	3.47	-0.9
H	0.015	1.085	+0.4

Table 2. Bond-stretching parameters for SiO_2 and hydroxylated SiO_2 surfaces.

Bond type	K_r (Kcal/mol Å^2)	$r_{0,ij}$ (e)
Si-O	285	1.68
O-H	495	0.945

Table 3. Angle-bending parameters for SiO_2 and hydroxylated SiO_2 surfaces.

Angle type	K_r (Kcal/mol rad^2)	θ_0 (°)
O-Si-O	100	109.5
Si-O-Si	100	149.0
Si-O-H	50	115.0

Table 4. Parameters (in real units) for TIP3P water model.

Type	Mass (g/mol)	Charge (e)	E (Kcal/mol)	σ (Å)
O	15.9994	-0.83	0.102	3.188
H	1.008	0.415	0	0

where the subscripts i, j, k denote atom indices; the first term describes van der Waals interactions via the 12-6 Lennard-Jones (L-J) potential with ε and σ as the energy and distance parameters and r_{ij} the interatomic separation; the second term is the Coulombic interaction using partial charges q and the vacuum permittivity ε_0; for 1-2 and 1-3 atom pairs within silica, L-J and Coulombic interactions are excluded; bond stretching and angle bending are modeled by harmonic potentials with parameters k_r, r_0 for bonds and k_θ, θ_0 for angles; the nonbonded parameters for SiO_2 and hydroxylated SiO_2 surfaces are listed in Table 1, bond-stretching and angle-bending parameters in Tables 2 and 3; nonbonded silica-water and water-water interactions use the same L-J/Coulombic forms; the TIP3P model is employed, with SHAKE constraining the O-H bond length to 0.9572 Å and the H–O–H angle to 104.52°, and complete TIP3P parameters provided in Table 4.

The 12-6 L-J interaction between different types of atoms can be calculated using the arithmetic mixing rule, as shown in Eqs. (2) and (3). The 12-6 L-J interaction is widely employed in a series of molecular dynamics simulations to describe the vdW interaction between silica and water, investigating the interfacial properties of silica-water systems. In summary, the silica-water interactions in our simulations consist of 12-6 L-J and Coulombic interaction, which have been carefully selected to reproduce various experimental properties, as studied in our previous work. For non-bonded vdW and Coulomb interaction, a cutoff radius of 12 Å is applied, and the long-range Coulomb interaction are calculated using the particle-particle particle-mesh algorithm with a precision of 1×10^{-6} (Ma et al., 2024):

$$\varepsilon_{sl} = \alpha\sqrt{\varepsilon_l \varepsilon_l} \tag{2}$$

$$\sigma_{sl} = \frac{\sigma_l + \sigma_s}{2} \tag{3}$$

2.2 Simulation analysis methods

2.2.1 Calculation of thermal boundary conductance

The TBC was calculated using the NEMD method (Sun et al., 2023):

$$\mathrm{TBC} = \frac{J}{A\Delta T} \tag{4}$$

where ΔT represents the temperature difference across the silica-water interface, which is calculated by extrapolating the linear fit of the temperature distribution in the water and silica regions to the interface. The positions of the first density peaks of silica and water closest to the interface are used to determine the location of the solid-liquid interface. A denotes the cross-sectional area of silica along the direction of thermal transport (x-y), and J is the heat flux generated in the direction of thermal transport (Sun et al., 2023):

$$J = \frac{Q_h + Q_c}{2\Delta t} \tag{5}$$

where Q_h and Q_c as the average energy input or output by the Langevin thermostat into the system during the operation time Δt, for the cold and hot regions, respectively. The J is calculated using the virial stress tensor form. Along the direction of thermal transport, the silica wall is divided into two parts based on the atomic position coordinates: $0 < z < 1.2$ nm and the remaining region. Atoms at the core act as heat sources to generate a stable heat flow, while water molecules in the outermost region act as cold sources. The silica is divided into two parts to avoid "false temperature jumps" at the boundaries when using the Langevin thermostat for temperature control, which could lead to inaccuracies in the calculated interfacial thermal conductance data. The calculation model is illustrated in Fig. 1(d).

2.2.2 Calculation of vibrational density of states

To elucidate the mechanisms underlying the enhancement of TBC at silica-water interfaces with varying hydroxyl densities, the atomic vibrational behavior of the system was investigated. Prior studies have suggested that a greater similarity in atomic vibrational characteristics can enhance interfacial

thermal exchange. The vibrational density of states (VDOS), which quantifies the intensity of phonon vibration modes across different frequencies, was calculated. The VDOS was determined through a fast Fourier transform of the velocity autocorrelation function (VACF) (Dickey and Paskin, 1969):

$$\mathrm{VDOS} = \int v(t)\exp(-2\pi i\nu t)\mathrm{d}t \tag{6}$$

where ν represents frequency, i is the imaginary unit, and γ denotes the VACF. The VACF can be obtained from the equation as follows: $\gamma(t) = \sum_i v_i(0)\cdot v_i(t)/\sum_i v_i(0)\cdot v_i(0)$, where $v_i(0)$ and $v_i(t)$ are the initial velocity and velocity of the atom at time t, respectively. In the calculation, the convergence of the VACF is monitored to determine the computational time for VDOS. After the simulation run exceeds 10 ps, the structure has reached the equilibrium stage.

2.2.3 Analysis of H-bonds dynamics

The time autocorrelation function of hydrogen bonds (H-Bonds) is utilized to characterize their dynamic behavior, with the calculation formula given in (Rapaport, 1983):

$$C(\tau) = \left\langle \frac{\sum h_{ij}(t_0)h_{ij}(t_0+t)}{\sum h_{ij}(t_0)^2} \right\rangle \tag{7}$$

where h_{ij} represents a binary measure of whether the pair of atoms ij forms a H-Bond, with $h_{ij}=1$ indicating the formation of a H-Bond and $h_{ij}=0$ indicating the absence of a H-Bond. A continuous lifetime definition is employed, where once a H-Bonds is broken, it is always considered as such, even if it forms again later.

The lifetime of the H-Bonds serves as an indicator of their stability and strength, and is calculated by:

$$\tau_x = \int_0^{\infty} \left(C(\tau) - \langle C(\tau)(t=\infty)\rangle\right) d\tau \tag{8}$$

The survival probability $S(t)$ of water molecules within the interfacial layer was calculated to ascertain the time scales for their presence at silica interfaces with different hydroxyl densities:

$$S(t) = \left\langle \frac{N(t,t+\tau)}{N(t)} \right\rangle \tag{9}$$

where N denotes the number of water molecules, t signifies the time step, and the angular brackets indicate the average over all starting times.

In addition, this study analyzed the orientation and charge distribution of water molecules at silica interfaces with varying hydroxyl densities to accurately delineate the layering of water molecules.

2.3 Simulation details

All simulations were performed using the open-source MD software LAMMPS (Thompson et al., 2022), with visualization of the results carried out through VMD (Humphrey et al., 1996). The total duration of the simulations was 10 ns. The computational procedure followed these stages: (1) Velocity initialization, where the velocities were adjusted to a temperature of 5 K; (2) Energy minimization to remove any artificially induced strains; (3) Equilibration of all systems in the isothermal-isobaric ensemble at 1 atm pressure and 333 K for 1 ns, ensuring proper water density; (4) Maintaining a constant temperature of 333 K for 5 ns using the Nosé-Hoover thermostat in the canonical ensemble to allow the system to equilibrate at the desired temperature; and (5) Conducting thermal transport simulations in the microcanonical ensemble for data collection. For the NEMD simulations, the system was divided into hot and cold regions, with the cold region set at 293 K and the hot region at 373 K. The simulation box was subdivided into 100 sections along the direction of thermal transport, and the average temperature in each section was recorded to create a temperature gradient. The thermal transport simulations ran for 4 ns, with the first 2 ns stabilizing the temperature and heat flux distribution, followed by 2 ns for statistical averaging, allowing for accurate measurement of the temperature gradient and heat flux, minimizing system randomness. Figs 1(c) and 1(d) display the typical temperature and heat flux profiles for silica-water systems with varying hydroxyl densities. The heat flux, J, was calculated by averaging the heat input in the cold region and the heat output in the hot region, as depicted in Fig. 1(c). The slope of the heat flux density curve, which reflects structural stability, was used to compute the TBC via Eq. (4). Periodic boundary conditions were applied in all three dimensions to mitigate boundary effects. A time step of $\Delta t = 1$ fs was selected, with atom positions and velocities updated using the standard Velocity-Verlet algorithm (Chen et al., 2020). Data were collected every 1,000 time steps.

During the thermal transport simulation phase, trajectory data were periodically sampled. Specifically, trajectory and velocity data were recorded every 100 simulation steps to facilitate further analysis of H-bonds, water density, and the orientation of water molecules. For post-simulation analysis, custom TCL and Python scripts were utilized to process the obtained trajectory files.

3. Results and discussion

3.1 Interfacial thermal transport at varying hydroxyl densities

The temperature distribution between silica-water interfaces with varying silanol densities is shown in Fig. 2(a). Several key characteristics of the temperature distribution can be discerned from the figure. Initially, a distinct temperature reduction is observed at the interface between the regions affected and unaffected by the thermostat, which occurs in silica with varying hydroxyl densities. This artificial ITR induced by the thermostat is attributed to the phonon mismatch at the interface due to the dynamic rescaling by the thermostat. This artificial effect of the thermostat has been previously investigated in studies (Li et al., 2019; Ghatage et al., 2020), which indicated that the temperature gradient differs between the thermostat-influenced and non-influenced regions, depending on the system's temperature and heat flux. Detailed examinations of these aspects can be found in the literature (Li et al., 2019).

Thermal transport within the silica region is facilitated by the interatomic interactions that occur. It was observed that

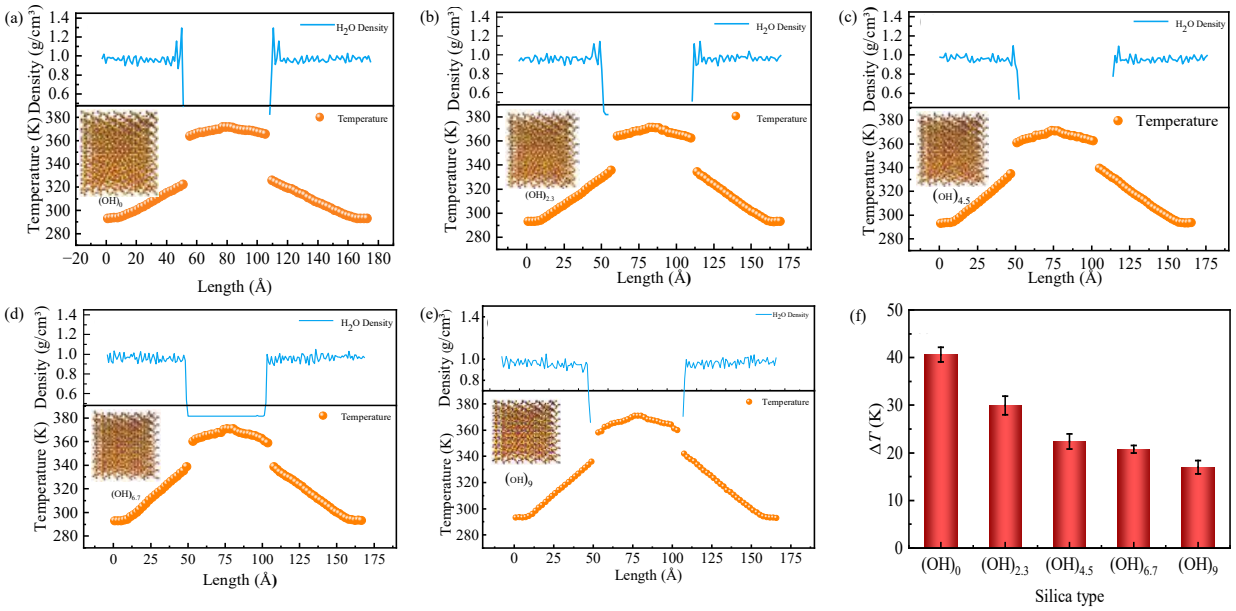

Fig. 2. Temperature and mass density distributions of silica-water systems with varying hydroxyl group densities: (a) $(OH)_0$, (b) $(OH)_{2.3}$, (c) $(OH)_{4.5}$, (d) $(OH)_{6.7}$, (e) $(OH)_9$ and (f) trend of temperature difference variation.

the temperature of silica exhibited a linear variation in regions distant from the thermostat-controlled area, whereas in its bulk region, the temperature change was relatively stable, with no significant temperature drop observed. However, the temperature decline in silica near the water region became more gradual, which is attributed to the scattering of the phonon at the interface. Furthermore, it was clearly noted that at the silica-water interface, due to the strong interactions between water and the solid material, the temperature fluctuations in the water near the solid surface were more pronounced than in the bulk water region, and these fluctuations diminished with increasing hydroxyl density, as depicted in Fig. 2(f). This trend in temperature variation has also been observed in our previous study on the thermal transport at interfaces of silica nanoparticles with varying wettability and water. The primary cause lies in the mismatch of atomic vibrations between the two media, leading to a temperature jump at the interface. This phenomenon was described by Oscar using a generalized acoustic model (Oscar et al., 2022). The TBC between silica and water with different hydroxyl densities was calculated using Eq. (4), based on the interfacial ΔT and J, with the results presented in Fig. 7(a). The figure illustrates that as the hydroxyl density on the silica surface increases, the ΔT at the interface gradually decreases, while the value of the TBC increases. This suggests that the presence of hydroxyl enhances the thermal transport capability between silica and water.

In investigating thermal transport at silica-water interfaces with varying hydroxyl densities, a significant temperature jump was observed, along with pronounced fluctuations in water density at the silica interface, peaking at a specific distance. Previous studies show that the TBC is closely related to fluid density at the solid interface (Lin et al., 2018), which aligns with earlier findings (Ma et al., 2024). To better understand the relationship between hydroxyl density, the interfacial temperature jump, and TBC, mass density variations of water at silica interfaces with different hydroxyl densities were calculated, as shown in Figs. 2(a)-2(e). The density distribution curves reveal an oscillatory pattern at the interface, forming two distinct peaks, with the first peak higher than the second. As the distance from silica increases, the water density distribution gradually returns to bulk water density. Additionally, as hydroxyl density increases, the first density peak decreases, and at the $(OH)_9$ interface, this peak disappears, resembling bulk water. In contrast, a distinct double-density peak is observed at the $(OH)_0$ surface. These density changes show a pattern opposite to temperature variations and interfacial thermal conductance changes.

The two-dimensional (2D) density distributions of water at silica-water interfaces with varying hydroxyl densities are shown in Figs. 3(a)-3(e). The results indicate the formation of a uniform density layer on all silica surfaces, along with a liquid depletion region at the interface. Hydroxyl groups influence the density distribution of water molecules on the silica surface, affecting the characteristic timescale for energy exchange between surface atoms and water molecules. At the $(OH)_0$ interface, water molecules display a banded distribution, whereas the presence of hydroxyls introduces linear depletion regions on the silica surface. Notably, at the $(OH)_{4.5}$ interface, pronounced density ripples are observed, caused by fluctuations in hydroxyl density, which trap more water molecules between the hydroxyl groups and the silica surface. This clustering of water molecules near the hydroxyls creates additional pathways for thermal transport, enhancing interfacial thermal conductivity. In contrast, at the $(OH)_9$ surface, water density fluctuations are less pronounced and follow a trend similar to that of one-dimensional mass density.

A previous study found that the interaction between Fe-

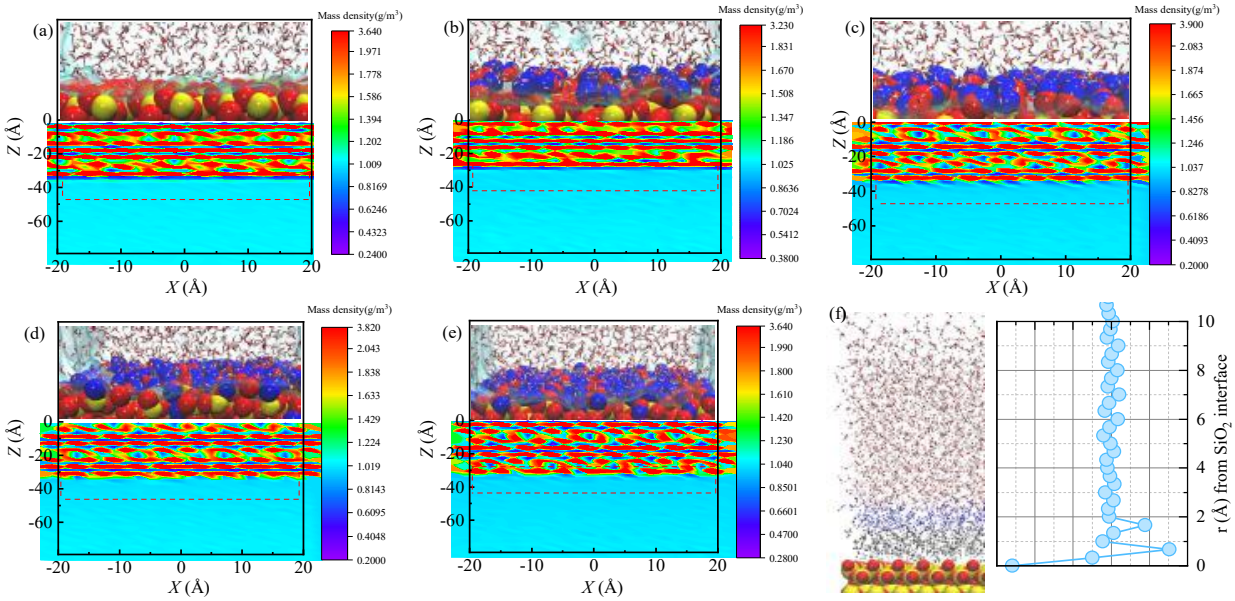

Fig. 3. 2D water density distribution: (a) $(OH)_0$, (b) $(OH)_{2.3}$, (c) $(OH)_{4.5}$, (d) $(OH)_{6.7}$, (e) $(OH)_9$ and (f) schematic diagram of the interfacial water layered structure.

H_2O nanoparticles leads to the formation of a "solid-like liquid layer" near the nanoparticle surface (Ma et al., 2024). In conditions of strong wettability, the density peak of water molecules at the nanoparticle interface is higher, indicating increased adsorption of water molecules, which results in a more compact structure. This layering phenomenon extends into the bulk water phase (Ma et al., 2024). Similarly, at the silica interface, surface forces at the nanoscale and liquid-liquid interactions also give rise to a "solid-like liquid layer" (Xue et al., 2004; Hamideh and Foroutan, 2017). Water molecules in this layer are more ordered than those in the bulk liquid, displaying crystalline-like characteristics. The presence of this special bimodal density peak or "solid-like liquid layer" facilitates thermal transport at solid-liquid interfaces. However, the current study shows that the introduction of hydroxyl groups at the silica interface disrupts the solid-like liquid structure. As the surface becomes more hydroxylated, the TBC increases. However, the "solid-like liquid layer" does not change in a linear manner and disappears entirely when the surface is fully hydroxylated. This suggests that the thermal transport mechanism at the silica-water interface, with varying hydroxyl densities, differs significantly from those at other solid-liquid interfaces.

3.2 Influence of hydroxyl density on the H-bonds dynamics of interfacial water

3.2.1 Solid-liquid interfacial H-bonds dynamics

H-bonds are primarily electrostatic interactions between H atoms, which are covalently bonded to a more electronegative atom or group (donor D), and an atom with a lone pair of electrons (acceptor A) that has a higher electronegativity (Emamian et al., 2019). This type of interaction is especially prominent due to the polar nature of water molecules.

The formation of H-bonds was determined based on geometric criteria, including the distance between the H atom and the acceptor atom (H···A), as well as the donor-hydrogen-acceptor (D-H···A) angle (Alosious et al., 2022). An H-bond is considered formed if the distance H···A is less than 3.5 Å and the angle D-H···A exceeds 150°, with the computational model depicted in Fig. 4(a) (Naveen et al., 2011). The dynamic behavior of H-bonds can be further explored by analyzing their number, lifetime, and time autocorrelation function under different hydroxyl densities.

Different types of the H-Bonds are formed between silica with varying hydroxyl densities and water, which are categorized as follows: (1) $SiO_2(O)\cdots(H)H_2O$, (2) SiO_2-$OH(H)\cdots(O)H_2O$, (3) SiO_2-$OH(O)\cdots$(H)-OH, (4) $SiO_2(O)^{Bulk}\cdots(H)H_2O$. Additionally, water molecules between the silica surfaces also form H-Bonds, as illustrated in Fig. 4(a). Previous studies have highlighted the importance of silica wall mobility in the formation and stability of surface H-bonds (Wang and Duan, 2015). In this study, however, no specific constraints were applied to the silica surface. As depicted in Fig. 4(b), a significant number of H-Bonds are formed between H_2O molecules near the interface and the silica surface, with the types of H-Bonds varying under different hydroxyl densities. The two predominant H-Bonds are 1) the strong H-Bonds formed by SiO_2-$OH(O)\cdots(H)H_2O$, suggesting that the H atom in the H_2O molecule is closer to the silica with varying hydroxyl densities, and (2) the H-Bonds formed by SiO_2-$OH(H)\cdots(O)H_2O$, where the O atom in the water molecule is closer to the silica. The number of these H-Bonds differs, with the number of SiO_2-$OH(O)\cdots(H)H_2O$ increasing as the hydroxyl density increases. The way the receptor and the donor atoms approach the silica with varying hydroxyl densities is fundamentally different, prompting us to analyze the dipole angle of the water molecules. Moreover,

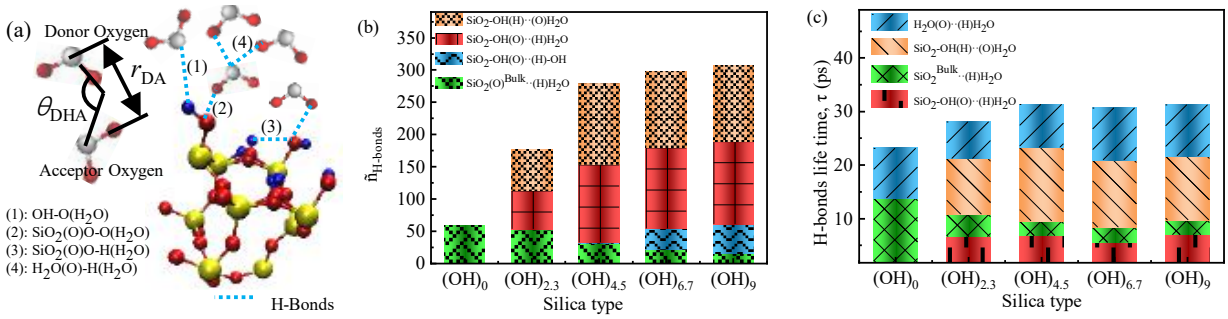

Fig. 4. (a) Criteria for H-bonds in this study, (b) number of H-bonds and (c) H-bond lifetime.

due to the considerable mobility of the hydroxyl on the silica interface, H-Bonds are also formed between the interfacial hydroxyl and O atoms in the bulk, and even between hydroxyl on the $(OH)_9$ interface. Consequently, the formation of H-Bonds at the silica interface involves a certain competitive mechanism.

The H-bonds between the silica interface and H_2O are dynamic, constantly breaking and reforming with different H_2O molecules. This dynamic process causes fluctuations in the system's dipole moment, which, in turn, influences the stability of the H-bond network responsible for thermal conduction. The average H-bond lifetime provides a measure of the rate at which these dynamic changes occur, and it is determined by fitting the time autocorrelation function. For bulk water, the calculated H-bond lifetime is $\tau = 1.60 \pm 0.02$, which aligns closely with the literature value of 1.66 (Duan et al., 2021). As illustrated in Fig. 4(c), the lifetimes of interfacial H-bonds between silica and water, with varying hydroxyl densities, show that the H-bonds formed between SiO_2-OH(H)···(O)H_2O have longer lifetimes, whereas other types of H-bonds exhibit relatively shorter lifetimes. As the hydroxyl density increases, the overall H-Bond lifetime at the interface also increases. A longer H-Bond lifetime suggests that, when a bond breaks, water molecules can rapidly form new H-Bonds with the silica surface, leading to a larger cluster of water molecules linked by H-Bonds. This process further strengthens the layered structure of water at the silica interface, contributing to a more stable and denser network within the adsorbed layer. Areas of higher water density facilitate the formation of additional H-bonds, which in turn improve structural stability and support the development of the H-bond network for thermal conduction, thus increasing the efficiency of thermal transport. These results are consistent with the findings of (Milischuk and Ladanyi, 2011), who investigated the diffusion behavior of water molecules in silica nanopores.

It is further noted that for the silica-water interface system with different hydroxyl densities, the average lifetimes of each H-Bonds type are different and do not exhibit a direct proportionality to the hydroxyl density. Related studies have indicated that various factors such as system temperature, hydroxyl area density, the confined state of the silica, and the arrangement of surface silanol can influence the structure of the interface's "solid-like liquid layer", which in turn affects the types of H-Bonds configurations and lifetimes, thus impacting interfacial thermal transport. To investigate the correlation between interfacial H-bonds dynamics and interfacial thermal transport, the structural characteristics of the "solid-like liquid layer" at silica interfaces with varying hydroxyl densities were first examined. This analysis was conducted to elucidate the microscopic mechanisms governing efficient thermal transport at the water-silica interface.

3.2.2 Distribution of H-bonds numbers along the direction of thermal transport

To better understand the structural properties of the "solid-like liquid layer" at silica interfaces with varying hydroxyl densities and its pivotal role in solid-liquid thermal transport, a thorough analysis of the H-bond distribution along the thermal transport direction was performed. In line with prior studies on H-bond formation at hydroxylated silica-water interfaces, the SiO_2-OH(O)···(H)H_2O H-bond type was found to be much more abundant than other types.

Related studies have shown that the interaction forces between H_2O-H_2O and H_2O-solid interfaces are comparable, facilitating the adsorption of randomly diffusing water molecules at hydroxyl-modified silica interfaces. Fig. 5(a) illustrates the distribution of the SiO_2-OH(O)···(H)H_2O pattern along the direction of thermal transport at silica-water interfaces with varying hydroxyl densities. As the hydroxyl density increases, the number of H-bonds in this pattern also increases, suggesting that more water molecules are anchored to the silica surface at the O atom, forming H-bonds. This enhances the formation of additional thermal transport channels at the silica interface, thereby increasing the probability of thermal transport. Moreover, it is apparent that with higher hydroxyl densities, the position at which this H-bonding pattern forms moves significantly farther from the silica surface. This is attributed to the unrestrained nature of surface hydroxyls, with the attraction between water molecules and hydroxyls after H-bond formation leading to this shift.

The water hexamer is regarded as the "minimal ice" structure, where its arrangement allows water molecules to align relatively flat against the metal surface, thereby optimizing the interaction between the water molecule and the metal. However, the formation of the ice-like bilayer structure occurs only when each water molecule is oriented so that a hydrogen atom points either toward or away from the surface, leading to the so-called H-down and H-up configurations. Previous

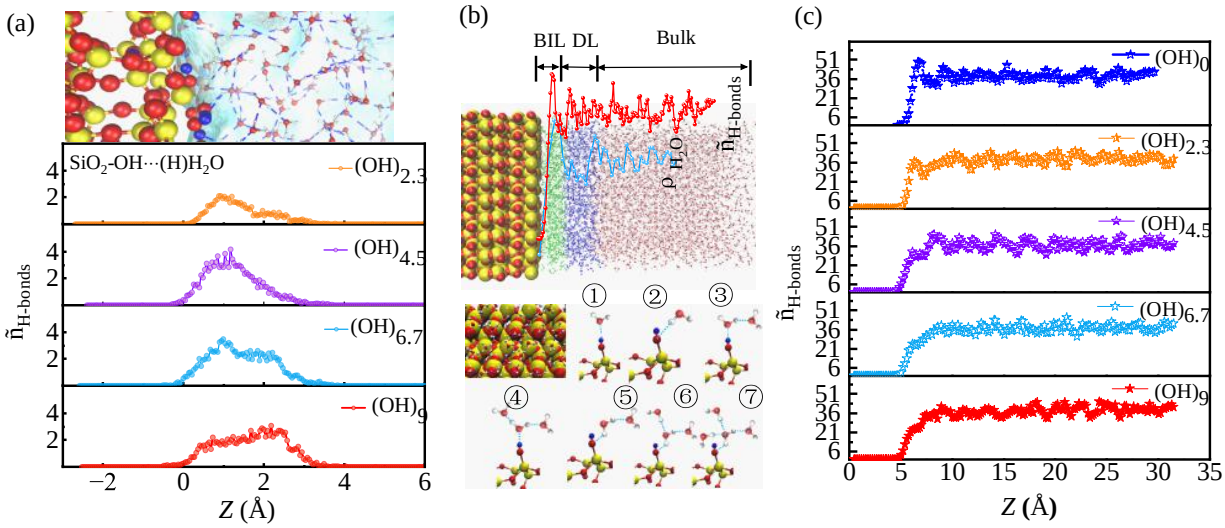

Fig. 5. (a) Number of $SiO_2-OH\cdots H_2O$ H-bonds, (b) structure of the adsorbed water bilayer and (c) number of water-water H-bonds.

studies on water molecule orientation show that as hydroxyl density increases, the formation of H-down structures becomes more prevalent at the silica interface, which increases the likelihood of water hexamer formation. Furthermore, as the hydroxyl density rises, each hydroxyl group can adsorb a maximum of one water molecule, resulting in monomeric adsorption.

Due to their polar nature, water molecules readily form H-bonds with neighboring molecules. The presence of hydroxyl groups at the silica interface disrupts the original H-bond network formed by water. To further understand the structural characteristics of the "solid-like liquid layer" at the silica interface and its relationship with thermal transport, the distribution of H-bonds formed by water molecules along the direction of thermal transport was analyzed, as shown in Fig. 5(c). The distribution of H-bonds closely follows the water molecule density distribution, both exhibiting a bilayer structure at the interface. However, the presence of hydroxyl groups disrupts this bilayer structure, especially at the $(OH)_9$ surface. Unlike the density distribution, the distribution of H-bonds and the bilayer pattern change more significantly with increasing hydroxyl density. Specifically, the bilayer structure of water molecules becomes less distinct as hydroxyl density increases. This is primarily due to interactions between water molecules in the interfacial layer and hydroxyl groups on the silica surface, which form a new H-bond network structure, disrupting the original water layer at the interface. As hydroxyl density increases, the H-bond distribution of water molecules shifts closer to the interface, with the first density peak moving nearer to the silica surface and showing reduced amplitude. This shift is a result of H-bonds forming between hydroxyl groups at the silica interface and water molecules. Previous orientation analyses show that in this scenario, water molecules are oriented perpendicularly at the silica interface, with the direction of H-bond formation aligned with the heat flow. This arrangement enhances the number of pathways available for heat transfer at the interface. The perpendicular alignment of water molecules in the confined space results in a reduced mass density at the interface. Additionally, the constraints imposed by the H-bonds further diminish the likelihood of random diffusive collisions among the water molecules, promoting increased interactions with the silica interface and favoring directed collisions.Consequently, the water molecule density and the first peak of the H-bond distribution decrease as hydroxyl density increases, while interfacial thermal conductivity rises.

3.3 Orientation and charge distribution of interfacial water molecules

Electrostatic repulsion is a key factor in the formation of the "solid-like liquid layer" at the solid-liquid interface. To gain a deeper insight into this structure at silica surfaces with varying hydroxyl densities, we analyzed the orientation and charge distribution of water molecules at the respective interfaces. The orientation of water molecules is influenced by their proximity to the surface and the surface characteristics, resulting in distinct orientation patterns. The orientation of interfacial water molecules is measured by the angle (Ψ) between the H_2O molecule's dipole moment and the direction perpendicular to the silica surface (Z-axis). Angles of 0° and 180° correspond to the OH bonds of the water molecule being directed away from or towards the surface, respectively, as shown in the schematic diagram in Fig. 6(c).

As shown in Fig. 6(a), which presents the orientation angles of water molecules at the silica interface with varying hydroxyl densities, the water molecules at the $(OH)_0$ interface display a uniform orientation distribution, with angles concentrated around 90°, indicating parallel alignment to the silica surface. As the hydroxyl density increases, the orientation of the water molecules shifts, showing a preference for alignment towards the silica surface. This preference is most noticeable within 3 Å of the interface, and as hydroxyl density increases,

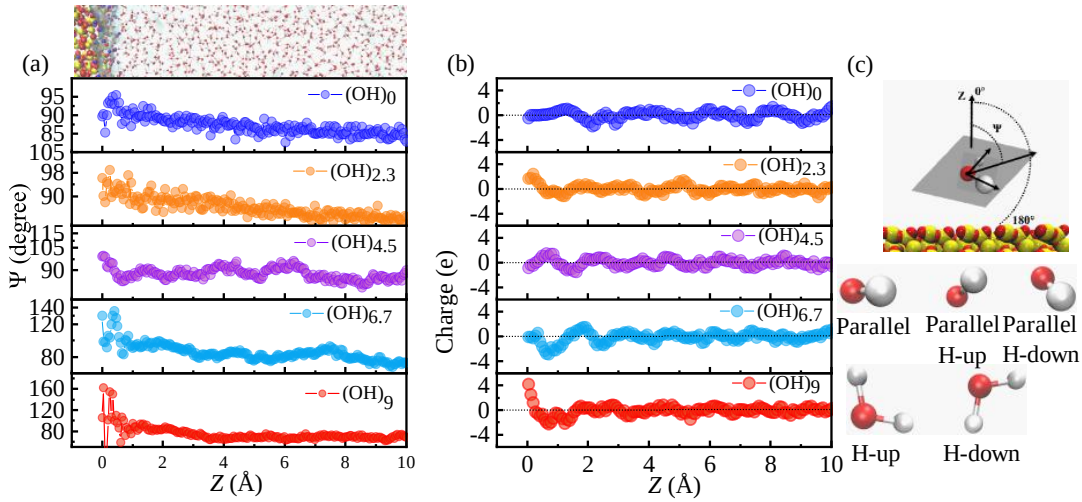

Fig. 6. (a) Orientation angle distribution, (b) charge distribution and (c) definition and calculation method for the water molecule orientation angle (Ψ).

the orientation becomes even more pronounced. At the $(OH)_9$ interface, the orientation of H_2O molecules is predominantly around 170°, suggesting that the hydrogen atoms of H_2O molecules are oriented towards the silica surface, forming H-bonds with the oxygen atoms. Additionally, a smaller proportion of water molecules show orientation angles less than 30°. These molecules contribute a hydrogen atom to form an H-bond with the oxygen atoms at the interface, leaving another hydrogen atom available for subsequent water molecules, resulting in an H-down orientation. In the $(OH)_9$ system, H_2O molecules in the adsorbed layer predominantly adopt the H-down state, with the H atoms closer to the silica than the O atoms. This indicates that surface hydroxyl groups encourage a vertical orientation of water molecules towards the silica surface, organizing their adsorption and disrupting the original interlayer structure of the water molecules.

Fig. 6(b) shows the charge distribution of water molecules at silica interfaces with varying hydroxyl densities. At these interfaces, the charge distribution forms a distinct bilayer structure, primarily due to the preferential alignment of water molecules at the silica surface. In the absence of hydroxyl groups, the dipole moment of the water molecules aligns with the interface normal, maintaining this bilayer electrostatic charge structure even on a horizontal interface. As the hydroxyl density increases, the bilayer structure becomes less pronounced, with the charge distribution following the trend of the water molecule density distribution.

3.4 Effect of hydroxyl density on thermal transport at silica-water interfaces

3.4.1 Analysis of interfacial potential energy

The interfacial potential energy is a critical factor in understanding variations in TBC (Sun et al., 2023). This energy is defined as the total interaction energy between the solid atoms and liquid molecules, normalized by the cross-sectional area in the direction of the heat flux. A lower interfacial potential energy generally corresponds to stronger solid-liquid interactions, which enhances heat transport across the interface. In this study, we investigated the influence of surface hydroxyl groups on the interfacial potential energy, which includes both vdW and Coulombic interactions. As shown in Fig. 7(b), introducing hydroxyl groups onto the silica surface significantly reduces this energy, aligning with the observed trend in TBC. The decrease in potential energy with increasing hydroxyl density is attributed to the enhanced accumulation of water molecules at the silica interface. These molecules interact more strongly with the surface, contributing more effectively to thermal transport, which simultaneously reduces the interfacial potential energy and increases TBC.

3.4.2 Dynamics of the interfacial bound water layer

Drawing from the insights of electrochemical studies on the organization of electrolyte structures, the layered structure of the "solid-like liquid layer" was further refined through the analysis of density distribution, water molecule orientation distribution, charge distribution, and the H-bonds formation. Upon obtaining the density distribution, a bilayer water structure at the silica interface was defined, as depicted in Fig. 3(f). This structure features a density peak approximately 3 Å from the silica interface, with a second peak appearing within the subsequent 5 Å range; the distribution of water molecules' H-bonds follows a similar pattern. From the standpoint of water molecule orientation, the interface adsorption layer comprises two adjacent sublayers: one with a specific orientation preference, representing a solid-like liquid water intermediate between the liquid and solid states, and the other without a specific orientation preference, representing liquid water. Based on these observations, the layered structure of the silica-water interface adsorption water layer was defined.

The arrangement of water at the first maximum of the density profile is strongly dictated by the physicochemical features of the silica surface and shows distinct dynamics as hydroxyl coverage changes. We refer to this interfacial layer as the BIL, which marks the primary region governing heat

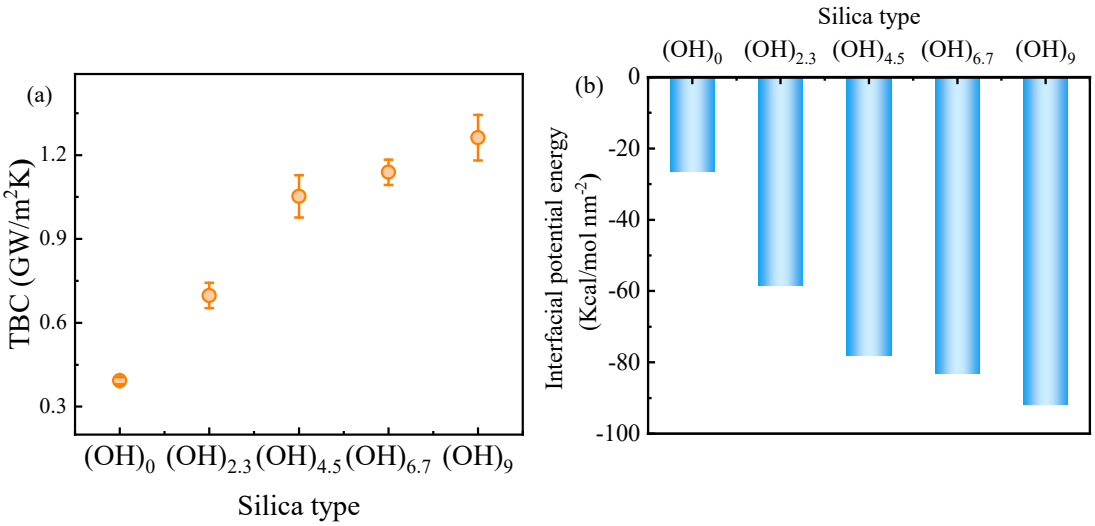

Fig. 7. Silica-water systems with varying hydroxyl group densities: (a) Interfacial thermal conductivity and (b) interfacial potential energy.

transfer across the solid-liquid boundary. The next maximum, located at ~5 Å from the surface, exhibits weak adsorption and no clear orientational preference, leading to higher mobility; this region is designated the DL, as shown in Fig. 5(b). We emphasize that resolving interfacial layering by molecular dynamics is nontrivial; in this work, the BIL and DL are defined strictly from the structural signatures of water.

Additionally, the dynamic behavior of the BIL and its correlation with thermal transport were analyzed, given that this layer is the first to interact with the heat emitted from the silica. The residence probability of water molecules, the number of H-bonds, and the VDOS spectrum within the BIL layer were examined. These analyses further clarified the relationship between the "solid-like liquid layer" structure and thermal transport performance.

The local translational and rotational mobility of water molecules is closely linked to their residence time within a specific region. To quantify this, the timescale for water molecules in the BIL layer was determined by calculating their survival probability at the silica interface. The survival probability, $S(t)$, indicates the likelihood that a water molecule in a given region at time $t = 0$ remains in the same region at a later time $t > 0$. The decay rate of $S(t)$ is influenced by both the size of the region and the mobility of the water molecules within it. Given a consistent calculation region, $S(t)$ is primarily related to the mobility of the water molecules. As shown in Fig. 8(a), $S(t)$ in the BIL layer is strongly affected by variations in surface hydroxyl density. For silica without hydroxyl coverage, $S(t)$ decreases by more than 50%. However, with complete hydroxyl coverage, the reduction in $S(t)$ is less significant. In the bulk water region, $S(t)$ converges quickly, indicating extremely fast mobility of water molecules in this region. This discrepancy arises because water molecules in the bulk are in constant motion, whereas in the BIL layer, the presence of hydroxyl groups creates a network of hydrogen bonds that restricts water mobility. As a result, water molecules in the BIL layer remain in place much longer than those in the bulk, reducing their diffusion potential. This confinement becomes more pronounced as hydroxyl density increases.

The total number of H-bonds and the average number per water molecule within the BIL layer are shown in Fig. 8(b). As the hydroxyl density increases, the total number of H-bonds in the BIL layer decreases, but this change does not show a simple linear correlation with the variation in interfacial thermal conductance. This result is understandable, given that hydroxyl groups disrupt the original structure of the water layer, pulling the H atoms of H_2O molecules towards the silica surface. In contrast, water molecules without hydroxyl coverage remain in a more planar configuration, which suggests a greater distance between the silica and water. Additionally, within the BIL layer, H_2O molecules contribute two H atoms each, forming H-bonds either with other water molecules in the BIL or in the DL layer. As a result, the total number of H-bonds in the BIL layer is reduced. Despite this, the reduction in H-bonds is compensated by an increase in the number of effective thermal transport paths, which leads to an enhancement of interfacial thermal conductance. Therefore, even with fewer H-bonds, the improved mobility of H_2O molecules in the BIL layer, especially with increasing hydroxyl density, helps increase the thermal transport efficiency.

3.4.3 Analysis of vibrational density of states

In the course of examining the thermal transport characteristics at silica-water interfaces with varying hydroxyl densities, it has been observed that interfacial potential energy and the H-bonds significantly influence the changes in the TBC. However, the more microscopic thermal transport mechanisms have yet to be fully elucidated. This situation calls for a more in-depth analysis of the microscopic mechanisms underlying interfacial thermal transport.

In previous analyses, it was found that due to the interaction of H-bonds, dense thermal transport channels were formed at the silica-water interface. Water molecules within the BIL

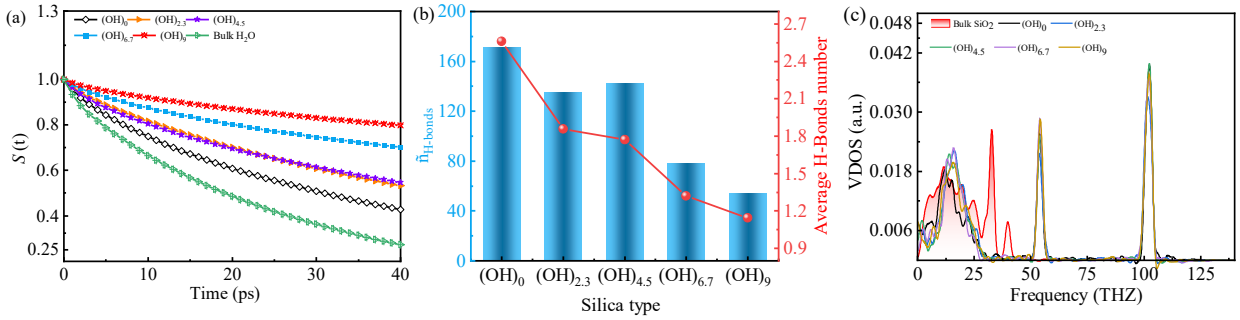

Fig. 8. (a) Survival probability of water molecules, (b) total number and average number of H-bonds, (c) VDOS of water molecules in the BIL layer.

close to the silica interface form H-bonds with hydroxyl, reducing the likelihood of random diffusion. Simulation of the vibrational dynamics at liquid-solid interfaces is a highly valuable tool for understanding thermal transport mechanisms. Therefore, the VDOS of interface atoms provides us with an important tool for understanding interfacial thermal transport. Fig. 9 presents the VDOS spectra of silica and water with different hydroxyl densities. It can be observed that there is a fundamental difference between the VDOS of water and silica, which is primarily due to their atomic structures. The mismatch in the VDOS of the two media leads to scattering of interface phonons, resulting in a temperature jump at the interface.

The VDOS spectrum for H_2O molecules exhibits three notable absorption peaks, each associated with specific molecular motions: torsional, oscillatory, and rotational movements. These peaks are indicative of the free movement of water molecules at 4.5 THz, the bending of the H−O−H bond at 7.9 THz, and the stretching of the O-H bond at 60.4 THz. Additionally, the O-H stretching mode is observed at 102 THz. The low-frequency range (5-30 THz) is characteristic of the vibrational modes within the hydrogen bond network of water molecules (Liu et al., 2009). The VDOS spectrum for silica is predominantly found in the low - frequency range (0-30 THz), with a pronounced peak near 34 THz. This peak suggests that the bulk atoms of silica vibrate vigorously at this frequency, generating thermal phonons and thus facilitating thermal transport. Additionally, recent research has shown that the vibrational modes in the VDOS of water molecules have diverse impacts on thermal transport efficiency. Furthermore, the low - frequency range of the VDOS is recognized as the critical frequency range for thermal transport within the thermal medium (Abhijith et al., 2023).

The VDOS spectrum of hydroxyl groups, shown in Fig. 9(b), is predominantly found in the low-frequency range, which can be attributed to the light mass of hydrogen atoms, producing a sharp peak around 40 THz. As surface hydroxyl density increases, the VDOS spectrum undergoes a noticeable shift: The peak at 13 THz diminishes gradually, while the peak at 40 THz broadens. This shift occurs because hydroxyl groups are in an amorphous state, leading to greater fluctuations compared to solid atoms. The vibrations of hydroxyl groups at the interface are significantly influenced by the interactions with silica and water, which affects their vibrational behavior. Additionally, the light mass of hydrogen atoms results in frequent vibrations at this low-frequency range. This frequency range corresponds to the vibrational modes of the H-bond network in water molecules.

The VDOS spectra for silica and water with varying hydroxyl densities are presented in Figs. 9(b)-9(e). It is indicated by the results that as the hydroxyl density increases, the VDOS spectra of both bulk water and the bare silica surface remain largely unchanged, with no significant shifts being observed. However, the VDOS spectrum of silica with hydroxyl coverage experiences frequency shifts and frequency multiplication, primarily due to the modification of silica's vibration properties by the hydroxyl. With the increase in hydroxyl density, the peak of the hydroxyl-covered silica VDOS spectrum at 30 THz gradually diminishes, while the peak at 40 THz increases. This diminishing is attributed to the fact that the frequency band in question is the vibration frequency band of the O atoms on the silica surface. As the hydroxyl coverage increases, it further suppresses the vibration of the O atoms, leading to the diminishment of phonons in that frequency band. The increase in the 40 THz band is mainly due to the vibration frequency range of the hydroxyl. As the hydroxyl density increases, the phonon vibration in this band is excited, further increasing the probability of thermal transport. Moreover, with the increase in hydroxyl density, it compensates for the mismatch in vibration between water molecules and silica in the low-frequency range (approximately 5-10 THz). The mismatch in atomic vibrations at the interface is reduced, leading to a higher degree of vibration coupling, further increasing the probability of energy transfer across the interface. Consequently, the TBC is significantly enhanced.

In conclusion, surface hydroxylation plays a crucial role in modifying the vibrational behavior of silica, thereby improving its thermal transport efficiency with water. However, the precise mechanism by which thermal energy is transferred from silica to the liquid phase remains unclear, likely due to the layered structure of water at the interface. To better understand the interfacial thermal transport mechanism, further detailed studies and analyses of this complex process are required.

The VDOS spectrum of water molecules in the BIL at silica interfaces with different hydroxyl densities is depicted in Fig. 8(c). Unlike bulk water, whose VDOS shows little

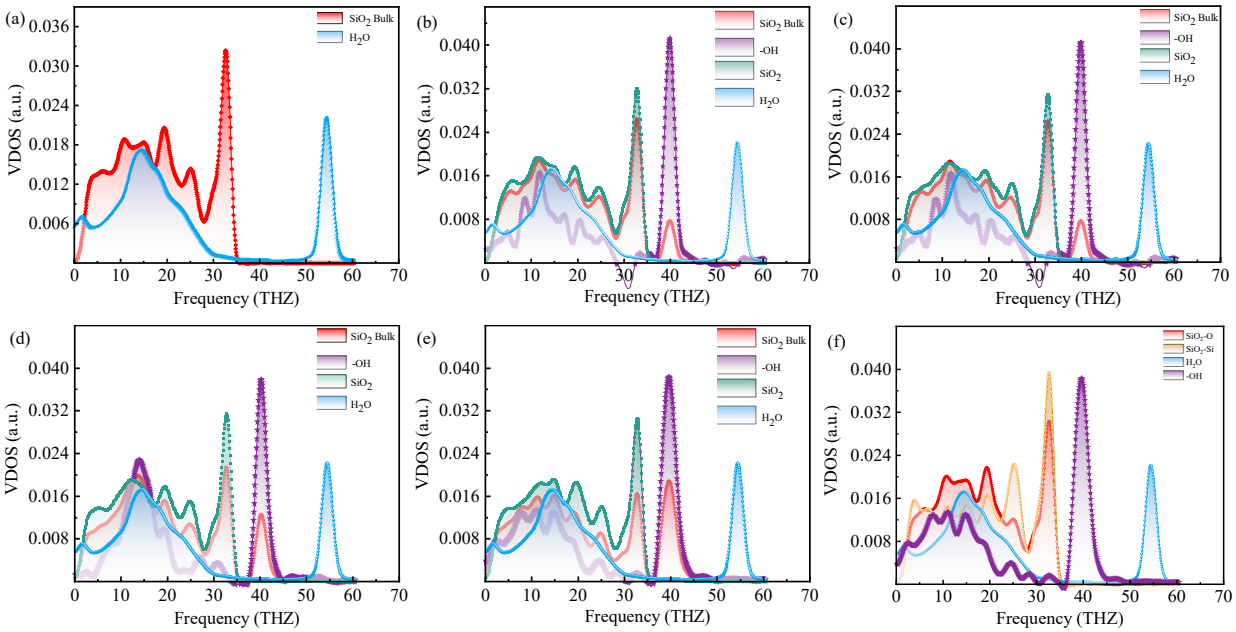

Fig. 9. VDOS for silica-water systems with different hydroxyl densities.

spectral shift, the VDOS of water molecules in the BIL is greatly affected by the interfacial environment. Specifically, as the hydroxyl density increases, the VDOS at 4.5 THz experiences a significant frequency shift. This shift indicates that the formation of H-bonds restricts the movement of water molecules in the BIL, thereby reducing their random diffusion. Due to the constraint of the SHAKE algorithm on bond angle stability, no significant changes are observed in the VDOS at 60.4 and 102 THz. Moreover, the collective vibrations of the H-bond network in the BIL cause a noticeable shift in the low-frequency VDOS range (0-30 THz), which is essential for thermal transport and corroborates our previous findings.

Fig. 8(c) reveals the phonon modes associated with interfacial heat transfer, which couple thermal energy from silica to the liquid phase. If an energy transfer pathway exists between silica and the liquid, the energy from these phonon modes is shared between both phases. Consequently, a shift in the VDOS frequency in the low-frequency range within the BIL layer is observed. However, in the absence of such a transfer channel, indicating weak interaction between the solid and liquid, phonon modes do not transfer energy from the solid to the liquid, causing the VDOS within the BIL to resemble that of a free surface. With increasing surface hydroxyl density, a blue shift in the VDOS peak at 10-15 THz is observed. This shift can be attributed to the formation of numerous hydrogen bonds between water molecules in the BIL layer and the surface hydroxyls on the silica, reducing the distance between water molecules and the silica surface. This results in limited movement of the water molecules, establishing a non-slip boundary condition. The vibration behavior of the BIL layer then becomes more similar to that of the silica wall, with the presence of hydroxyl groups further amplifying this effect. This phonon energy shift reflects the fundamental mechanism of thermal transport at the silica-water interface, which varies with different hydroxyl densities.

3.5 Microscopic mechanism of interfacial thermal transport

Through an in-depth investigation of the thermal transport mechanism, H-bonds have been identified as playing a pivotal role in the heat transfer process. A stable structure is formed by water molecules on the silica surface via H-bonds interactions. This structure not only enhances the vibrational coupling between the water molecules and the silica substrate but also significantly improves the efficiency of thermal transport. Furthermore, the presence of surface hydroxyl groups is found to strengthen these H-bonds interactions. The resulting increase in the number, stability, and lifetime of H-bonds collectively contributes to the enhancement of interfacial thermal conductance. Based on these observations, it is inferred that an efficient channel for thermal energy transport is established at the silica-water interface, as illustrated in Fig. 10. Finally, a fitting analysis of the interfacial thermal conductance as a function of hydroxyl density was performed, yielding the following quantitative relationship: $y = -0.001029x^3 - 0.0392x^2 + 0.390x + 0.384$.

Within this transmission channel, heat is initially generated by the vibration of silica bulk atoms, which excites phonons that carry the heat from the silica bulk. However, at the interface between silica and water, due to the mismatch of vibration modes, not all the heat carried by phonons can be effectively transmitted, leading to scattering of phonons at the interface and causing a temperature jump. Thanks to the presence of hydroxyl, numerous H-bonds form between the silica surface and water molecules, limiting the movement of water molecules and extending their residence time on the silica surface, thereby strengthening the vibration coupling effect. During this process, the water molecules in the BIL

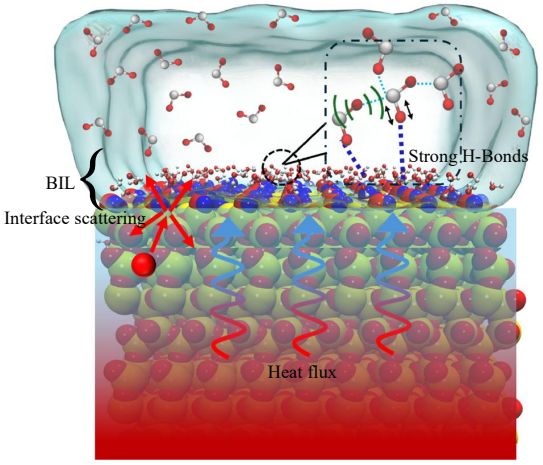

Fig. 10. Thermal transport mechanisms at the silica-water interfac.

at the silica interface act as the key medium for thermal energy transfer. The vertical arrangement of BIL layer water molecules aids in the more distant and effective transmission of thermal energy. On the other hand, on the silica surface without hydroxylation, water molecules tend to be parallelly arranged, lacking effective thermal transfer paths, resulting in a significant temperature jump at the interface. In contrast, at the silica-water interface with complete hydroxyl coverage, a smaller temperature gradient indicates effective thermal transport along the direction of the thermal flow through H-bonds interactions. It can thus be concluded that thermal transport originates in the silica bulk, then proceeds through the hydroxyl groups, and ultimately reaches the water molecules in the BIL layer via intermolecular interactions. Subsequently, the water molecules in the BIL layer transfer heat energy to the DL through vibrational and collisional effects. Finally, heat energy is further propagated within the DL layer through diffusion to more distant water regions.

Furthermore, there may be some structural or dynamic differences that are not evident from the current analysis, leading to inaccuracies in the understanding of the layered structure at the silica interface. In any case, future research should give due consideration to the impact of this layered effect on the more intricate mechanisms of interfacial thermal transport.

4. Conclusions

In conclusion, the present study utilized molecular dynamics simulations to examine the thermal transport properties of silica-water interfaces across a spectrum of hydroxyl densities, with an emphasis on elucidating the roles of interfacial H-bonds and stratified structures. It was observed that the TBC at the silica-water interface escalates in tandem with the augmentation of surface hydroxyl density. This augmentation is predominantly ascribed to the hydrogen-bonded thermal conduction network that materializes around the silica. Upon scrutinizing the water density, H-bonds distribution, charge distribution, and molecular orientation at the silica interface, a dual-layer model encompassing the DL and the BIL was formulated. Within the BIL, the structure of water molecules is modulated by the presence of surface hydroxyl groups, thereby curtailing their mobility and engendering a vibrational dominance in thermal transport within this stratum. Moreover, as the hydroxyl density ascends, the interfacial potential energy diminishes, permitting a greater number of water molecules to adsorb onto the silica interface in an H-down configuration. The prevalence of hydroxyl groups catalyzes the formation of an abundance of H-bonds between the silica surface and water molecules, which in turn restricts their movement, prolongs their residence time, and ushers in additional thermal pathways. This study not only augments the fundamental comprehension of thermal transport at solid-liquid interfaces but also furnishes practical guidance for optimizing the thermal performance of nanofluid materials and thermal management materials. Future endeavors could holistically contemplate a gamut of intermolecular forces, especially weak interactions, to uncover the intricate motion and interaction mechanisms of water molecules within the interfacial layer, thereby offering a more holistic perspective on the microscopic processes of interfacial thermal transport.

Acknowledgements

The authors are grateful to Yunnan Fundamental Research Projects (No. 202301AT070469) and Yunnan Major Scientific and Technological Projects (No. 202202AG050002).

Conflict of interest

The authors declare no competing interest.

References

Abhijith, A., Bladimir, R. A., Kannam, S. K., et al. Effects of interfacial molecular mobility on thermal boundary conductance at solid-liquid interface. The Journal of Chemical Physics, 2023, 158(9): 094710.

Alosious, S., Kannam, S. K., Sathian, S. P., et al. Effects of electrostatic interactions on kapitza resistance in hexagonal boron nitride-water interfaces. Langmuir, 2022, 38(29): 8783-8793.

Bahiraei, M., Monavari, A., Moayedi, H. Second law assessment of nanofluid flow in a channel fitted with conical ribs for utilization in solar thermal applications: effect of nanoparticle shape. International Journal of Heat and Mass Transfer, 2020, 151: 119387.

Barisik, M., Beskok, A. Temperature dependence of thermal resistance at the water/silicon interface. International Journal of Thermal Sciences, 2014, 77: 47-54.

Bourg, I. C., Steefel, C. I. Molecular dynamics simulations of water structure and diffusion in silica nanopores. The Journal of Physical Chemistry C, 2012, 116(21): 11556-11564.

Chen, J., Xu, X., Zhou, J., et al. Interfacial thermal resistance: Past, present, and future. Reviews of Modern Physics, 2022, 94(2): 025002.

Chen, T., Zhou, S., Hu, Z., et al. A multifunctional superhydrophobic melamine sponge decorated with Fe_3O_4/Ag nanocomposites for high efficient oil-water separation and antibacterial application. Colloids and Surfaces A: Physicochemical and Engineering Aspects, 2021, 626: 127041.

Chen, Y., Yu, B., Zou, Y., et al. Molecular dynamics studies of bubble nucleation on a grooved substrate. International Journal of Heat and Mass Transfer, 2020, 158: 119850.

Dickey, J. M., Paskin, A. Computer simulation of the lattice dynamics of solids. Physical Review, 1969, 188(3): 1407-1418.

Duan, T., Yan, S., Zhao, Y., et al. Relationship between hydrogen bond network dynamics of water and its terahertz spectrum. Acta Physica Sinica, 2021, 70(24): 248702.

Emami, F. S., Puddu, V., Berry, R. J., et al. Force field and a surface model database for silica to simulate interfacial properties in atomic resolution. Chemistry of Materials, 2014, 26(8): 2647-2658.

Emamian, S., Lu, T., Kruse, H., et al. Exploring nature and predicting strength of hydrogen bonds: A correlation analysis between atoms-in-molecules descriptors, binding energies, and energy components of symmetry-adapted perturbation theory. Journal of Computational Chemistry, 2019, 40(32): 2868-2881.

Gao, S., Bao, X., Yu, L., et al. Molecular dynamics study of "quasi-gemini" surfactant at n-decane/water interface: the synergistic effect of hydrophilic headgroups and hydrophobic tails of surfactants on the interface properties. Colloids and Surfaces, A: Physicochemical and Engineering Aspects, 2022, 634: 127899.

Ghatage, D., Tomar, G., Shukla, R. K. Thermostat-induced spurious interfacial resistance in non-equilibrium molecular dynamics simulations of solid-liquid and solid-solid systems. The Journal of Chemical Physics, 2020, 153(16): 164110.

Hamideh, B. K., Foroutan, M. Water distribution in layers of an aqueous film on the titanium dioxide surface: A molecular dynamic simulation approach. Journal of Molecular Liquids, 2017, 244: 291-300.

Hu, M., Goicochea, J. V., Michel, B., et al. Thermal rectification at water/functionalized silica interfaces. Applied Physics Letters, 2009, 95(15): 151903.

Huang, H., Zhong, Y., Cai, B., et al. Size- and temperature-dependent thermal transport across a Cu-diamond interface: Non-equilibrium molecular dynamics simulations. Surfaces and Interfaces, 2023, 37: 102736.

Huang, X., Liu, R., Liu, Z. Evaporation of ultra-thin water film on hot spot with nanopillar array. International Journal of Thermal Sciences, 2022, 182: 107807.

Humphrey, W., Dalke, A., Schulten, K. VMD: Visual molecular dynamics. Journal of Molecular Graphics, 1996, 14(1): 33-38.

Idumah, C. I., Obele, C. M. Understanding interfacial influence on properties of polymer nanocomposites. Surfaces and Interfaces, 2021, 22: 100879.

Jin, J., Wang, X., Wick, C. D., et al. Silica surface states and their wetting characteristics. Surface Innovations, 2020, 8(3): 145-157.

Kapitza, P. L. Heat Transfer and Superfluidity of Helium II. Physical Review, 1941, 60(4): 354-355.

Kieu, H. T., Liu, B., Zhang, H., et al. Molecular dynamics study of water evaporation enhancement through a capillary graphene bilayer with tunable hydrophilicity. Applied Surface Science, 2018, 452: 372-380.

Kodama, T., Shinohara, N., Hung, S. W., et al. Modulation of interfacial thermal transport between fumed silica nanoparticles by surface chemical functionalization for advanced thermal insulation. ACS Applied Materials & Interfaces, 2021, 13(15): 17404-17411.

Li, Z., Xiong, S., Sievers, C., et al. Influence of thermostatting on nonequilibrium molecular dynamics simulations of heat conduction in solids. The Journal of Chemical Physics, 2019, 151(23): 234105.

Liang, C., Yasin, A., Zhang, L., et al. Solar interfacial evaporator with three-dimensional architecture for seawater desalination. Colloids and Surfaces, A: Physicochemical and Engineering Aspects, 2024, 702: 135035.

Lin, T., Li, J., Quan, X., et al. A molecular dynamics investigation on effects of nanostructures on thermal conductance across a nanochannel. International Communications in Heat and Mass Transfer, 2018, 97: 118-124.

Liu, J., Miller, W. H., Paesani, F., et al. Quantum dynamical effects in liquid water: A semiclassical study on the diffusion and the infrared absorption spectrum. The Journal of Chemical Physics, 2009, 131(16): 164509.

Ma, M., Zhang, X. H., Qing, S., et al. Wettability-dependent thermal transport at the Fe nanoparticle-water interface: molecular dynamics simulations. Journal of Molecular Liquids, 2024, 402: 124717.

Martínez, L., Andrade, R., Birgin, E. G., et al. PACKMOL: A package for building initial configurations for molecular dynamics simulations. Journal of Computational Chemistry, 2009, 30(13): 2157-2164.

Milischuk, A. A., Ladanyi, B. M. Structure and dynamics of water confined in silica nanopores. The Journal of Chemical Physics, 2011, 135(17): 174709.

Morishige, K. Influence of Pore Wall Hydrophobicity on Freezing and Melting of Confined Water. The Journal of Physical Chemistry C, 2018, 122(9): 5013-5019.

Naveen, M., Woolf, T. B., Beckstein, O. MDAnalysis: A toolkit for the analysis of molecular dynamics simulations. Journal of Computational Chemistry, 2011, 32(10): 2319-2327.

Oscar, G.-V., Merabia, S., Santamaria, R. Size-dependent effects of the thermal transport at gold nanoparticle-water interfaces. The Journal of Chemical Physics, 2022, 157(8): 084702.

Pezzotti, S., Galimberti, D. R., Gaigeot, M.-P. Deconvolution of BIL-SFG and DL-SFG spectroscopic signals reveals order/disorder of water at the elusive aqueous silica interface. Physical Chemistry Chemical Physics, 2019, 21(40): 22188-22202.

Pittenger, B., Fain, S. C., Cochran, M. J., et al. Premelting at ice-solid interfaces studied via velocity-dependent indentation with force microscope tips. Physical Review B,

2001, 63(13): 134102.

Qi, Y., Feng, Q., Huang, X., et al. Hydrophobic composite phase change coating: Preparation, performance and application. Colloids and Surfaces A: Physicochemical and Engineering Aspects, 2024, 702: 135156.

Rapaport, D. C. Hydrogen bonds in water: Network organization and lifetimes. Molecular Physics, 1983, 50(5): 1151-1162.

Schoen, P. A. E., Michel, B., Curioni, A., et al. Hydrogen-bond enhanced thermal energy transport at functionalized, hydrophobic and hydrophilic silica-water interfaces. Chemical Physics Letters, 2009, 476(4): 271-276.

Sun, H., Surblys, D., Cheng, S., et al. Molecular dynamics study on the effect of surface ionization on the interfacial heat transfer between silica and water. Applied Thermal Engineering, 2024, 244: 122762.

Sun, H. Y., Surblys, D., Matsubara, H., et al. Molecular dynamics study on the role of hydrogen bonds and interfacial heat transfer between diverse silica surfaces and organic liquids. International Journal of Heat and Mass Transfer, 2023, 208: 124091.

Thompson, A. P., Aktulga, H. M., Berger, R., et al. LAMMPS – a flexible simulation tool for particle-based materials modeling at the atomic, meso, and continuum scales. Computer Physics Communications, 2022, 271: 108171.

Uchida, S., Fujiwara, K., Shibahara, M. Structure of the water molecule layer between ice and amorphous/crystalline surfaces based on molecular dynamics simulations. The Journal of Physical Chemistry B, 2021, 125(33): 9601-9609.

Ueki, Y., Matsuo, S., Shibahara, M. Molecular dynamic study of local interfacial thermal resistance of solid-liquid and solid-solid interfaces: Water and nanotextured surface. International Communications in Heat and Mass Transfer, 2022, 137: 106232.

Wang, B., Xu, Z., Wang, X., et al. Molecular dynamics investigation on enhancement of heat transfer between electrified solid surface and liquid water. International Journal of Heat and Mass Transfer, 2018, 125: 756-760.

Wang, C., Xing, Y., Zhang, C., et al. Water structure at coal/water interface: insights from SFG vibrational spectroscopy and MD simulation. Colloids and Surfaces, A: Physicochemical and Engineering Aspects, 2024, 688: 133604.

Wang, M., Duan, F. Effect of interfacial hydrogen bonds on the structure and dynamics of confined water. Acta Physica Sinica, 2015, 64(21): 218201.

Wang, Y., Keblinski, P. Role of wetting and nanoscale roughness on thermal conductance at liquid-solid interface. Applied Physics Letters, 2011, 99(7): 073112.

Wu, X., Han, Q. Tunable anisotropic in-plane thermal transport of multilayer graphene induced by 2D empty space: Insights from interfaces. Surfaces and Interfaces, 2022, 33: 102296.

Xue, L., Keblinski, P., Phillpot, S. R., et al. Effect of liquid layering at the liquid-solid interface on thermal transport. International Journal of Heat and Mass Transfer, 2004, 47(19-20): 4277-4284.

Zhang, L., Su, Q. Performance manipulations of a composite membrane of low thermal conductivity for seawater desalination. Chemical Engineering Science, 2018, 192: 61-73.

Zhao, J., Tian, S., Jiang, Z., et al. Study on the mechanism of SiO_2-H_2O nanofluid enhanced water injection in coal seam. Applied Surface Science, 2024, 658: 159843.